Anal. Chem. 1997, 69, 3321−3328

On-Line Detection of Nonspecific Protein Adsorption at Artificial Surfaces

Robert Ros Seigel, Philipp Harder, Reiner Dahint, and Michael Grunze*

Angewandte Physikalische Chemie, Universität Heidelberg, Im Neuenheimer Feld 253, 69120 Heidelberg, Germany

Fabien Josse*

Department of Electrical and Computer Engineering and Microsensor Research Laboratory, Marquette University, P.O. Box 1881, Milwaukee, Wisconsin 53201-1881

Milan Mrksich† and George M. Whitesides

Department of Chemistry, Harvard University, Cambridge, Massachusetts 02138

A detailed understanding of the interaction of proteins with artificial surfaces is essential for many applications in medicine and biochemistry. The affinity of surfaces toward proteins may, for instance, remove pharmacological proteins from media or control the adherence of pathogenic bacteria to protheses. Only a few analytical techniques now exist that can be used to study the binding process in real time, using unlabeled proteins. By investigating the adsorption kinetics of fibrinogen at differently terminated self-assembled monolayers (SAMs) of alkanethiols on thin gold films, it is demonstrated that acoustic plate-mode sensors are a promising analytical tool for studying the adsorption of proteins. In agreement with previous studies for fibrinogen, it is shown in situ that hexa(ethylene glycol)-terminated SAMs ($HS(CH_2)_{11}(OCH_2CH_2)_6OH$) exhibit very low protein adsorption and that methyl-terminated SAMs ($HS(CH_2)_{11}CH_3$) tend to adsorb large amounts of protein nonspecifically. The observed adsorption kinetics deviate from classical Langmuir behavior; these kinetics are compatible with a mechanism that involves an unfolding of fibrinogen after adsorption. Film quality is controlled by IR, XPS, and contact angle measurements.

A detailed understanding of the interactions of proteins with artificial surfaces is essential for many medical and biochemical applications.[1,2] Examples of the interaction of artificial surfaces with proteins include adsorption of proteins on catheters, protheses, and storage vessels in contact with biological fluids[3] and adhesion of pathogenic bacteria to prostheses.[4] A fast analytical tool capable of examining the adsorption of proteins at these surfaces would aid in understanding the mechanisms of these processes and support technological progress. Surfaces with well-defined characteristics are also required in order to create general model systems for studying the effects of surface properties on protein adsorption.

Several sensor technologies exist and have been used for real-time, on-line monitoring of biospecific interactions. Each method offers some specific advantages such as time resolution,[5] spatial resolution,[6] or the detection of protein self-exchange processes.[7] Biosensors based on the surface plasmon resonance (SPR) use changes in the index of refraction at the sensor surface due to adsorption of protein.[8] Acoustic wave-based sensors are sensitive to mass deposition at the sensing surface ("mass loading") and changes in the viscoelastic, electric, and dielectric properties at the sensor/liquid interface.[9,10] Thus, different physical parameters are accessible using SPR and acoustic wave technology. Acoustic wave sensors are suitable for time-resolved in situ measurements and can be manufactured in large quantities at low costs. In situ measurements of protein adsorption kinetic and protein coverage require no multistep separation and modification procedures of the analyte such as the covalent attachment of fluorescent dyes[6] for total internal reflection fluorescence (TIRF) or radiolabeled iodine[7] for γ-counting experiments. For routine analyses, the experimental setup is simple and requires only electronic circuits be integrated into the system; no laser beam (TIRF, ellipsometry) or external analyzers such as γ-counters is needed.

In the case of corrosive analytes, the use of acoustic plate mode (APM) devices has proved to be a promising concept, since sensor electrodes and analyte are strictly separated. Moreover, this class

† Present address: The University of Chicago, Chicago, IL.

(1) Horbett, D. J., Brash, J. L., Eds. *Proteins at Interfaces II: Fundamentals and Applications*; ACS Symposium Series 602; American Chemical Society: Washington, DC, 1995.
(2) Chuang, H. Y. K. Interaction of Plasma Proteins with Artificial Surfaces. In *Blood Compatibility*; Williams, D. F., Ed.; CRC Press: Boca Raton, FL 1987; Vol. 1, pp 87−102.
(3) Sluzky, V.; Tamada, J. A.; Klibanov, A. M.; Langer, R. *Proc. Natl. Acad. Sci. U.S.A.* **1991**, *88*, 9377−9381.
(4) Norde, W.; Lyklema, J. *Colloids Surf.* **1989**, *38*, 1−13.
(5) Malsten, M.; Lassen, B. In *Proteins at Interfaces II*; Horbett, T. A., Brash, J. L., Eds.; ACS Symposium Series 602; American Chemical Society: Washington, DC, 1995; pp 228−238.
(6) Ho, C.-H.; Hlady, V. In *Proteins at Interfaces II*; Horbett, T. A., Brash, J. L., Eds.; ACS Symposium Series 602; American Chemical Society: Washington, DC, 1995; pp 371−384.
(7) Huetz, P.; Schaaf, P.; Voegel, J.-C.; Mann, E. K.; Miras, B.; Ball, V.; Freund, M.; Cazenave, J.-P. In *Proteins at Interfaces II*; Horbett, T. A., Brash, J. L., Eds.; ACS Symposium Series 602; American Chemical Society: Washington, DC, 1995; pp 334−349.
(8) Malmqvist, M. *Nature* **1993**, *361*, 186−187.
(9) Nieuwenhuizen, M. S. Mass-Sensitive Devices. In *Sensors*; Göpel, W., et al., Eds.; VCH: Weinheim, 1991; Vol. 2.
(10) Grate, J. W.; Martin, S. J.; White, R. M. *Anal. Chem.* **1993**, *65*, 940−948, 987−996.

S0003-2700(97)00047-4 CCC: $14.00

of sensors allows on-line and direct detection of label-free proteins, thus saving time and providing the opportunity to study the kinetics of the binding process.[11,12] By miniaturizing the sensor elements, only a small amount of analyte is required for the analysis. Perturbation of the crystal surface caused by physical or chemical interactions, such as protein adsorption, results in a change of the wave propagation characteristics, i.e., frequency and/or attenuation of the acoustic mode. In the case of thin films, the change in frequency has been shown to be a direct function of the mass bound at the sensing surface.[13]

On the basis of previous work,[14,15] oligo(ethylene glycol)-terminated self-assembled alkanethiol monolayers (SAMs) should exhibit low protein adsorption, and methyl-terminated SAMs tend to adsorb a monolayer (or more) of proteins nonspecifically. In the present study, APM sensors have been used to investigate the binding processes at these SAMs on-line and to determine the characteristics of protein adsorption. A kinetic model has been developed that can account for the experimentally observed nonspecific adsorption processes. In order to improve the performance of the sensor, the APM device utilizes a new design with different interdigital transducer (IDT) structures as input and output. A dual-delay line configuration was used in order to compensate for secondary effects and to compare directly the adsorption behavior of differently derivatized crystal surfaces.

EXPERIMENTAL SECTION

Sensor Design. An IDT radiates energy into a semiinfinite piezoelectric medium. In the case of a thin parallel crystal plate, the radiated bulk wave energy sets up APMs at different frequencies. For a given crystal orientation, the structure of the APM spectrum is determined by the ratio of plate thickness, h, and IDT period, λ.[16] For high h/λ values, i.e., at high frequencies of operation, the spectrum becomes very dense. Consequently, the dominant signal is distorted by adjacent modes. This distortion limits both the accuracy and reproducibility of the measurements and the achievable detection limits.[17] Thus, new sensor designs are required to overcome this problem.

Figure 1 shows an improved concept to reduce mode interference by the use of differently shaped transmitter and receiver IDTs. It utilizes the fact that IDTs can be operated at different harmonics. If the transmitter IDT is designed with four fingers per period (4F-IDT) and the receiver IDT with three fingers per period (3F-IDT), a situation is obtained where the transmitter is exciting the fundamental frequency and odd harmonics, while the receiver is detecting the fundamental frequency and even harmonics. By selecting the ratio of the individual fundamental frequencies such that one or more harmonics of the dominant modes coincide, and adjacent modes interfere destructively (see, for example, Figure 1), spurious sensor response is drastically reduced.

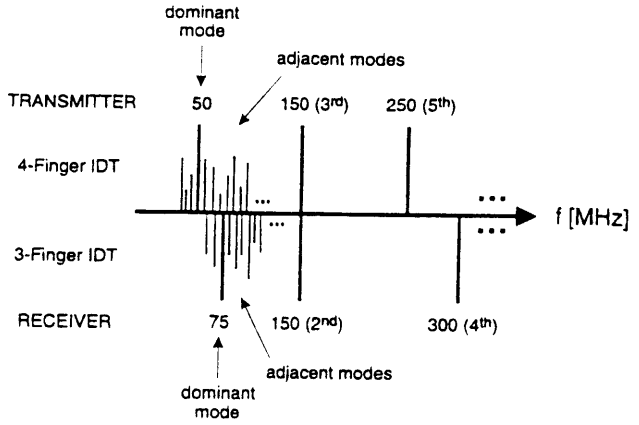

Figure 1. Improved sensor design utilizing a 4F-IDT for the transmitter and a 3F-IDT for the receiver. The lines represent the various modes excited (or received) by each IDT. While the transmitter is exciting the fundamental frequency and odd harmonics, the receiver is detecting the fundamental frequency and even harmonics. If the ratio of the individual fundamental frequencies is selected such that one or more harmonics of the dominant modes coincide and adjacent modes interfere destructively, spurious sensor response can be significantly reduced.

For a practical implementation of this concept, a large number of APM spectra were numerically calculated[17] and a promising combination of transmitter and receiver IDT was selected. The parameters chosen were $\lambda = 92.0$ μm for the 4F-IDT and $\lambda = 61.2$ μm for the 3F-IDT. On 0.5 mm thick ZX-$LiNbO_3$—the selected crystal orientation and thickness—these values correspond to fundamental frequencies of about 48 and 72 MHz, respectively. In order to eliminate acoustoelectric interactions with the analyte[18] and to facilitate the formation of thiol SAMs, the upper crystal surface was sputtered with a 20 nm adhesive layer of Cr and 60 nm of Au. For the metal deposition, the substrates were kept at room temperature. Sputtering rates of 100 nm/h and 200 nm/h were used for Cr and Au film formation, respectively. The device is operated at ~145 MHz where the second harmonic response of the 3F-IDT and the third harmonic response of the 4F-IDT coincide.

Figure 2 presents a comparison of the conventional 4F/4F design (a, b) and the new 4F/3F design (c, d). The spectra in (a) and (c) represent nonfiltered data while the spectra in (b) and (d) are obtained by numerically removing electromagnetic crosstalk and spurious adjacent modes, so-called "gating". Although the frequency of operation—and thus the value of h/λ—is almost the same, the nonfiltered data of the 4F/3F design yield a much better sensor response. Only after removing spurious signals by gating did the quality of the two responses become the same. On the basis of these results, the newly designed sensor element (4F/3F) was selected for all of the on-line adsorption studies described below. A dual-delay line configuration was used in order to compensate for secondary effects and to compare directly the adsorption behavior of differently derivatized crystal surfaces.

Chemicals. Ethanol (Baker, AR), H_2O_2 (Baker, 30%), H_2SO_4 (Riedel-de Haën, 95–97%), sodium dodecyl sulfate (SDS, Serva, >99.9%), and 1-dodecanethiol (Sigma) were used as received. (1-Mercaptoundec-11-yl)hexa(ethylene glycol) [$HS(CH_2)_{11}(OCH_2$-

(11) (a) Dahint, R.; Grunze, M.; Josse, F.; Renken, J. *Anal. Chem.* **1994**, *66*, 2888–2892. (b) Andle, J. C.; Vetelino, J. F.; Lade, M. W.; McAllister, D. J., *Sens. Actuators B* **1992**, *8*, 191–198.

(12) Renken, J.; Dahint, R.; Grunze, M.; Josse, F. *Anal. Chem.* **1996**, *68*, 176–182.

(13) Bender, F.; Dahint, R.; Josse, F.; Grunze, M.; v. Schickfus, M. *J. Acoust. Soc. Am.* **1994**, *95*, 1386–1389.

(14) Prime, K. L.; Whitesides, G. M. *J. Am. Chem. Soc.* **1993**, *115*, 10714–10721.

(15) Mrksich, M.; Sigal, G. B.; Whitesides, G. M. *Langmuir* **1995**, *11*, 4383–4385.

(16) Wagers, R. S. *IEEE Trans. Sonics Ultrason.* **1976**, *SU-23*, 113–127.

(17) Josse, F.; Dahint, R.; Schumacher, J.; Grunze, M.; Andle, J. C.; Vetelino, J. F. *Sens. Actuators A* **1996**, *53*, 243–248.

(18) Dahint, R.; Grunze, M.; Josse, F.; Andle, J. C. *Sens. Actuators B* **1992**, *9*, 155–162.

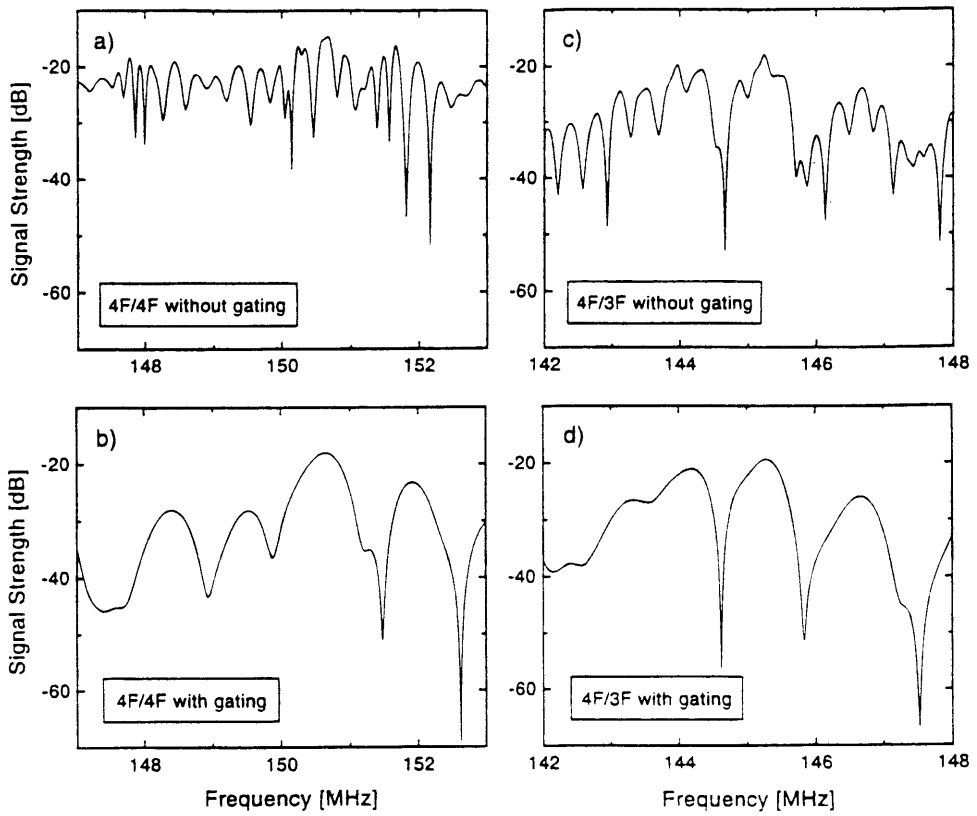

Figure 2. Comparison of the conventional 4F/4F design (a, b) and the new 4F/3F design (c, d). For almost the same frequency of operation the nonfiltered data of the 4F/3F structure yield a drastically improved sensor response (a, c). Only if spurious signals are numerically removed by gating (b, d) is the same signal quality obtained for the two responses.

$CH_2)_6OH$] was synthesized at Harvard University.[19] Bovine albumin fraction V [BSA, assay (CAF) >99%, 11924] was bought from Serva. Phosphate-buffered saline (PBS, P-4417), fibrinogen (F-4883, ~50% protein, 20% sodium citrate and ~30% NaCl, ~94% clottability), and ribonuclease A (RNA, R-5125) were bought from Sigma. Catalog numbers are indicated in parentheses. Throughout the experiments, PBS was used at pH 7.4.

As high concentrations of fibrinogen dissolved only slowly in PBS, the fibrinogen solutions were allowed to stand overnight and filtered through 0.22 μm hydrophilic cellulose acetate membrane filter units (Model C450.1, Carl Roth GmbH, 76185 Karlsruhe, Germany) before use. The actual concentrations of the dissolved fibrinogen were determined by comparison of the UV absorption at 214 nm with the absorption of 0.1‰ RNase A and 0.1‰ BSA solutions. At this wavelength, the absorption of proteins was found[20] to be almost independent of pH in the range from 4 to 8. Also, the variation in amino acid composition of different proteins has relatively little effect on the absorption values, as the low wavelength used is primarily detecting absorption by peptide bonds. The absorption of a filtered 0.1‰ solution of the raw product (~50% fibrinogen, sodium citrate, NaCl) was ~45% of the absorption of the reference solutions. Hence, the relative loss of fibrinogen in the filter was ~10%. It should be noted that all quantities refer to proteins equilibrated in ambient atmosphere and not to "dry" proteins; as much as 10% of the weighed material is likely to be water, and the quantity of proteins used in these experiments is uncertain to that extent.

Film Preparation and Characterization. For the sensor experiments, the nonelectrode surface of the APM devices was sputtered with a 20 nm adhesive layer of Cr, followed by 60 nm of Au. The thiol monolayers were prepared under ambient conditions in a single-chamber Teflon cell, which was mounted on top of the devices covering both sensing and reference lines. First, the gold surface was cleaned for 15 min in a freshly prepared 1:3 mixture of H_2O_2 and H_2SO_4 cooled to 50 °C (caution: this so-called piranha solution reacts violently, even explosively, with organic materials).[21] The cell was next rinsed 10 times with ultraclean water (Millipore) and blown dry with nitrogen. Deposition of 1-dodecanethiol was performed on both sensing and reference lines by filling the cell with 2 mL of a 5 mM thiol solution in ethanol for 12 h. Upon removal of this solution, the cell was rinsed several times with ethanol and water. After a nitrogen blow dry, crystal and cell were tilted and 50 °C hot piranha solution was added dropwise onto the reference line. As determined by XPS, an incubation time of 15 min is sufficient to remove the organic film completely. After extensively rinsing the reference line with Millipore water and a nitrogen blow dry, the bare gold region was derivatized by incubation with a 5 mM hexa(ethylene glycol)-terminated alkanethiol $[HS(CH_2)_{11}(OCH_2CH_2)_6OH]$[19] solution in ethanol for 1 h. Finally, the whole Teflon cell was rinsed several times with ethanol and Millipore water.

To check the film quality, some larger (1.5 × 2.5 cm^2), nonelectrode samples were prepared under the same conditions and examined with X-ray photoelectron spectroscopy and FT-IR spectroscopy. XPS spectra of these films were found to be in good

(19) Pale-Grosdemange, C.; Simon, E. S.; Prime, K. L.; Whitesides, G. M. *J. Am. Chem. Soc.* **1991**, *113*, 13–20.

(20) Thorne, C. J. R. Techniques for determining protein concentration. In *Techniques in Protein and Enzyme Biochemistry*; Kornberg, H. L., et al., Eds.; Elsevier: New York, 1978; B 104/2.

(21) Dobbs, D. A.; Bergman, R. G.; Theopold, K. H. *Chem. Eng. News* **1990**, *68* (17), 2. (b) Wnuk, T. *Chem. Eng. News* **1990**, *68* (26), 2. (c) Matlow, S. L. *Chem. Eng. News* **1990**, *68* (30), 2.

agreement with previous reports.[19] A single alkyl C 1s signal was observed for the methyl-terminated thiol monolayer while C 1s spectra of the hexa(ethylene glycol)-terminated SAM yielded two peaks at 285.0 and 286.7 eV. The latter corresponds to methylene groups adjacent to an oxygen atom (OCH_2). Oxygen (not detectable in the 1-dodecanethiol film spectra) shows an O 1s band at 533 eV.

IR spectra of both monolayers were obtained in external reflection (~80° angle of incidence) using p-polarized light. In the spectral range from 3000 to 2800 cm^{-1}, the methyl-terminated SAMs are characterized by the presence of five distinct C−H stretching bands. Three of them, namely, those at 2965, 2939, and 2850 cm^{-1}, correspond to the methyl group (antisymmetric and symmetric stretch with its Fermi resonance splitting component). The other bands at 2920 and 2850 cm^{-1} can be assigned as due mainly to contributions from the methylene C−H antisymmetric and symmetric stretching modes, respectively.[22] These peak positions correspond to those reported for all-trans extended chains and suggest that the chains are embedded in a crystalline-like environment. The relative weakness of the methylene bands compared with the methyl bands (band height $CH_{3\text{-sym}} > CH_{2\text{-sym}}$) indicates a preferential chain axis orientation normal to the surface. Thus, the methylene stretches have their main component parallel to the surface and can interact only weakly with the electric field. IR spectra from hexa(ethylene glycol)-terminated SAMs showed a broad band between 2950 and 2830 cm^{-1} due to overlapping C−H stretching modes of the methylene groups adjacent to oxygen and to the methylene groups of the $(CH_2)_{11}$ tail.

Static advancing contact angle measurements with water resulted in 38 ± 2° for the hexa(ethylene glycol)-terminated SAM and 107 ± 2° for the methyl-terminated SAM, respectively. The latter contact angle lies between the values of 114° reported for a close-packed methyl surface and 102° reported for a methylene-terminated surface. Measurements with hexadecane yielded values of 41 ± 2°, close to the literature value of 46° for a methyl surface.

APM Sensor Measurements. In order to avoid corrosion problems, the APM device is mounted with the IDTs on the bottom surface. A liquid cell of ~0.5 mL volume is fixed on the upper side to expose a well-defined region of the sensing surface to the solution. A flat rubber gasket is used to provide a liquid-tight seal. Afterward, the sensor is inserted into a temperature-controlled isolation box with an integrated flow system as shown in Figure 3. The latter consists of two liquid tanks containing the solutions used in the measurements and a container for waste. A peristaltic pump ensures continuous sample delivery at a controlled flow rate of ~0.6 mL/min. Two three-way valves determine whether liquid is pumped from tank 1 or 2 and whether the solution is directed into the waste or back to tank 2. All components are mounted on a copper plate to provide good thermal contact. In order to avoid experimental error due to temperature gradients, the APM device and the solutions in the tanks were maintained at the same controlled temperature. The measurements were performed at 25 °C with temperature variations of less than ±0.2 °C.

All experiments followed the same procedure. PBS was allowed to flow through the cell and then substituted with a flow

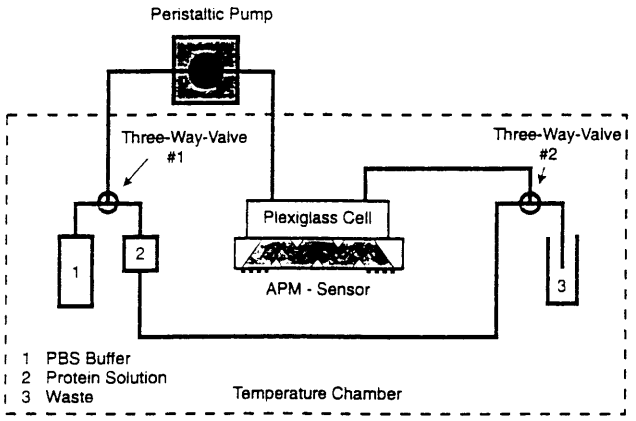

Figure 3. Block diagram of the continuous-flow system.

of the protein solution. In order to restrict the amount of analyte used, three-way valve 2 was switched such that the solution is pumped back into tank 2 after 5 min for the experiments shown in Figure 6, and after 10 min for the studies of Figures 5 and 7. After the sensor response reached an equilibrium state, valve 2 was switched back to its initial position and the protein solution was replaced by PBS. For the regeneration of the sensing surface, a solution of SDS (1% per weight in PBS at pH 7.4), was pumped through the liquid cell using again tank 2, followed by a neat buffer flow from tank 1.

For all measurements, phase and signal amplitudes of the electrical output of the APM device are compared to the input of the sensor as a function of the binding process. By the use of two miniature relays, both sensing and reference lines can be monitored separately. In order to determine the relative signal changes due to protein adsorption, the response of the PBS-covered sensor is taken as the reference. Before the experiments, the phase-frequency characteristics of the two lines are determined to convert the observed phase shifts into corresponding frequency changes. Single line responses are temperature-corrected using the experimentally determined frequency−temperature characteristics (FTC) of 76 ppm/°C.[18]

As shown in Figure 4, two electronic setups can be used for signal analysis, a network analyzer and a combination of signal generator and vector voltmeter. The network analyzer provides the opportunity to eliminate signal distortion due to electromagnetic feedthrough and adjacent modes by digital signal processing. Thus, baseline stability and reproducibility of the measurements is enhanced. However, the underlying mathematical operations are rather time-consuming, and the time required to measure sensing and reference lines separately is ~25 s. By contrast, the combination of signal generator and vector voltmeter does not provide any filtering of the sensor response but can be used to study the binding process at time intervals of ~5 s. The two electronic measurement systems have been described in detail elsewhere.[18,23] Since this study emphasizes quantitative data analysis and accurate comparison of the sensor response under different experimental conditions, the use of the network analyzer was preferred. A Pt100 thermometer was mounted at the bottom of the device to monitor temperature changes. The entire measurement was automated using a personal computer.

(22) Laibinis, P. E.; Whitesides, G. M.; Allara, D. L.; Tao, Y.-T.; Parikh, A. N.; Nuzzo, R. G. *J. Am. Chem. Soc.* **1991**, *113*, 7152−7167.

(23) Schumacher, J.; Dahint, R.; Josse, F.; Grunze, M. *IEEE Ultrason. Symp.* **1994**, 629−632.

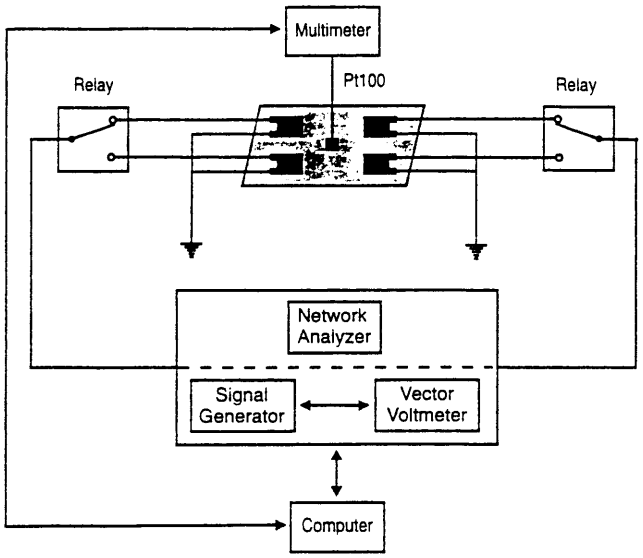

Figure 4. Block diagram of the electronics measurement setup. For signal analysis, the sensor element can be connected either to a network analyzer or a combination of signal generator and vector voltmeter. Two relays allow monitoring of the sensing and reference lines separately. Temperature is measured with a Pt100 and read out with a digital multimeter.

RESULTS AND DISCUSSION

Continuous Flow Measurements. For the on-line detection of protein adsorption, the sensing line of the APM device was coated with hydrophobic, methyl-terminated SAMs [$HS(CH_2)_{11}$-CH_3], and the reference line with hexa(ethylene glycol)-terminated SAMs [$HS(CH_2)_{11}(OCH_2CH_2)_6OH$]. Figure 5 shows the affinity of the two lines toward protein adsorption. After signal stability under PBS was monitored for 10 min, the surface of the sensor was exposed to a 28 μg/mL fibrinogen solution in PBS. While no signal change was observed for the reference line, the signal line showed a frequency decrease of ~400 Hz. The small drift in the single line responses may be explained by the fact that the frequency–temperature characteristics of the coated device differ slightly from the value of 76 ppm/°C,[18] which was experimentally determined for a noncoated sensor and used to correct the measured data for temperature variations. The above results confirm in an on-line experiment that pristine hexa(ethylene glycol)-terminated SAMs exhibit very low protein adsorption but that methyl-terminated SAMs adsorb large amounts of protein nonspecifically. This observation is in good agreement with previous studies using ex situ spectroscopy[14] and in situ surface plasmon resonance analysis.[15] We conclude that a hexa(ethylene glycol)-coated sensor line is an excellent reference for further experiments, since protein adsorption is effectively suppressed. An absolute measure of the amount of adsorbed proteins is difficult, because sensor response is not only a function of the adsorbed mass but also of the coupling between the proteins and the sensing surface.[12] Therefore, independent calibration measurements would be necessary for a quantitative analysis. As the scope of the studies was to directly compare the adsorption characteristics at different artificial surfaces and not to quantify the adsorbed mass, no such effort has been made.

Noting that hexa(ethylene glycol)-terminated SAMs are inert to protein adsorption, the following experiments were focused on the difference in the response of the two lines. If the difference signal, defined as sensing line minus reference line response, is considered, secondary effects, such as temperature changes, are effectively eliminated from the sensor response without any numerical computation.

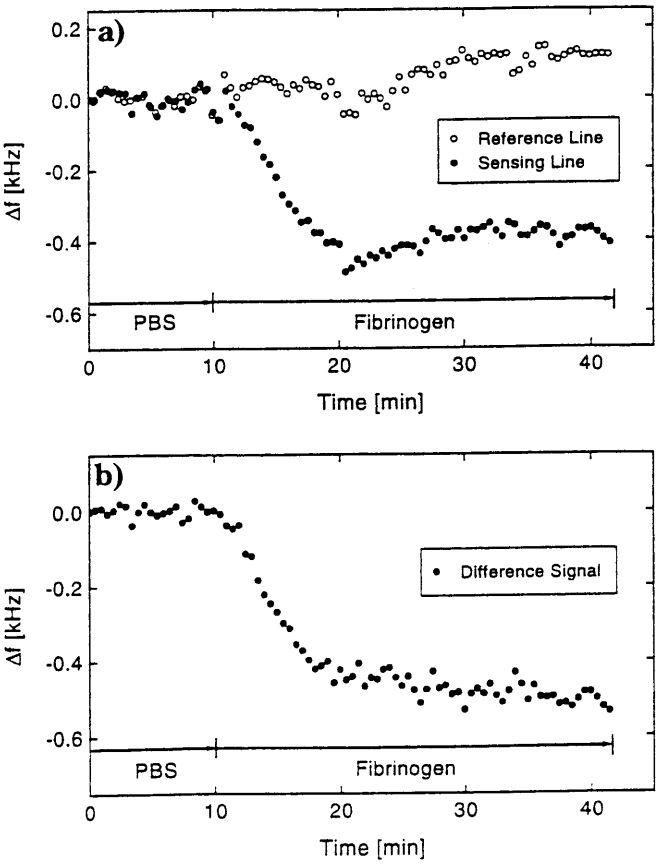

Figure 5. On-line detection of protein adsorption. The sensing line of the APM device was coated with 1-dodecanethiol, the reference line with a hexa(ethylene glycol)-terminated SAM. After 10 min, the continuous-flow system was switched from PBS to a fibrinogen solution at a concentration of 28 μg/mL. While no binding processes are observed for the reference line, the signal line shows a frequency decrease of ~400 Hz due to nonspecific protein adsorption. (a) Individual behavior of the two lines. (b) Sensing line minus reference line response (difference signal).

In order to determine whether protein adsorption at the methyl-terminated SAMs is reversible, a 800 μg/mL fibrinogen solution was pumped through the liquid cell. As shown in Figure 6, a fast frequency decrease of ~700 Hz is obtained. Flushing the cell with PBS reduces the sensor response only by ~120 Hz, indicating that the main portion of fibrinogen has been irreversibly attached to the methyl-terminated line. By using SDS and a subsequent wash with PBS solution, all proteins are removed from the surface and the sensor returns to its initial state. Successful regeneration of the sensor surface has been demonstrated for fibrinogen concentrations down to 3 μg/mL. Again, these observations are in good agreement with SPR analysis.[15] They suggest that one coated sensor element can be used for a complete set of experiments. Thus, possible systematic errors due to slightly different mass sensitivities of the devices or minor differences in the quality of the coatings can be effectively reduced.

Figure 7 presents measurements of the sensor response as a function of fibrinogen concentrations ranging from 3 to 280 μg/mL. Figure 8 summarizes the observed steady state frequency shifts at long times after fibrinogen adsorption. In principle, two relatively simple explanations can be given for the data presented in this figure. First, this kind of behavior will be observed for

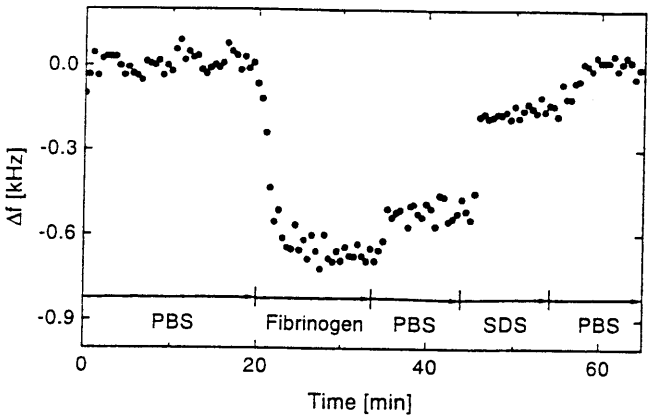

Figure 6. After the stability of the sensor is monitored for 20 min, it is exposed to a 800 μg/mL fibrinogen solution. Subsequent flushing with PBS only removes a small portion of the adsorbed proteins. However, by the use of SDS and PBS, the sensor element can be completely regenerated.

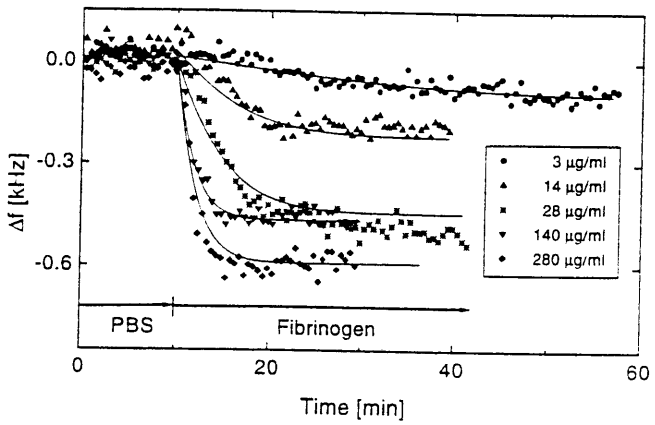

Figure 7. Sensor response as a function of protein concentration. Adsorption of fibrinogen is monitored for different concentrations of protein. It is observed that frequency shifts at equilibrium strongly depend on protein concentration. The solid lines show a fit to the experimental data according to eqs 6 and 9.

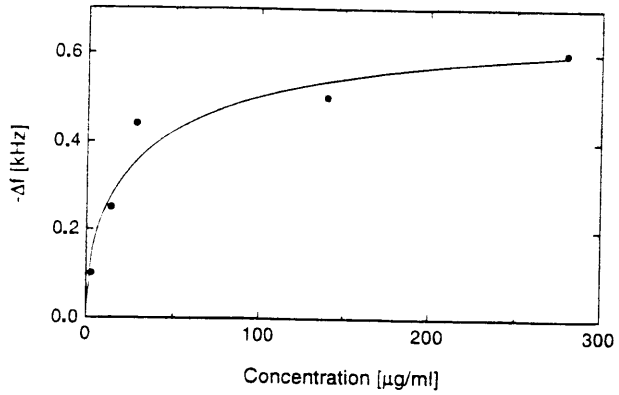

Figure 8. Frequency shifts at equilibrium for the experiment shown in Figure 7. The solid line is a fit to the experimental data using eqs 8 and 9.

the equilibrium states of a reversible adsorption/desorption process as described by a Langmuir isotherm. The fact (Figure 6) that large amounts of protein are irreversibly bound to the sensor surface obviously contradicts the assumptions of this model. The second explanation is based on the hypothesis that adsorbed proteins can unfold at the surface of the SAM and occupy larger surface areas than they will when adsorbed in the native state. As protein concentrations increase, the adsorption

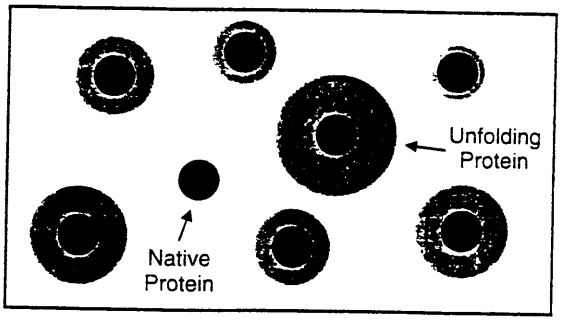

Figure 9. Schematic picture of the adsorption process: Proteins adsorbing onto an artificial surface will cover a relatively small area (black circles) as long as they maintain their native state. Due to the unfolding process, additional surface area is occupied (gray rings).

process might happen sufficiently rapidly so that the surface would be completely covered with protein molecules before a significant fraction of them could unfold. Thus, at high concentrations, a larger number of proteins would bind to the surface than at low concentrations. The adsorbed film at high concentrations would be a monolayer of approximately native proteins; at low concentrations, it would be a monolayer of spread and denatured proteins. The former would be thicker.[24]

Kinetic Model of the Adsorption Process. In an effort to determine whether the second approach can account for the observed data, the following kinetic model was developed: As shown in Figure 9, native proteins may adsorb from solution onto an artificial surface. Just as for Langmuir kinetics, the adsorption rate is assumed to be proportional to the concentration, c, of proteins in solution and to the free surface area. This relationship may be expressed by

$$d\theta_1/dt = k_a c(1 - \theta) \quad (1)$$

where $\theta = \theta_1 + \theta_2$ denotes the fraction of surface area covered with proteins ($0 \le \theta \le 1$). It is composed of θ_1, which is the area that would be occupied if all proteins were still in their initial state (black circles in Figure 9), and θ_2, which is the increase in covered area due to the unfolding process (gray rings in Figure 9). The rate constant for adsorption is k_a. For most surface experiments and all experiments carried out here, the amount of protein in solution is large compared to the amount on the surface. Under these conditions, c is constant and $k_a c$ is a pseudo-first-order rate constant with units of reciprocal seconds. Note that θ_1 is proportional to the number of adsorbed proteins.

After adsorption, it is assumed that the proteins will unfold at a rate that is proportional to the number of adsorbed molecules and to the noncovered surface area:

$$d\theta_2/dt = k_u \theta_1(1 - \theta) \quad (2)$$

Here, k_u is the rate constant at which unfolding occurs. For the sake of simplicity it is assumed that the unfolding process is only limited by the available surface area and not by any restrictions due to the actual size of the molecules. We regard this simplification to be acceptable, provided the surface coverage is not too low. We emphasize that both k_a and k_u have to be interpreted as average rate constants for a heterogeneous ensemble of fibrinogen

(24) Ramsden, J. J. *Chem. Soc. Rev.* **1995**, 73–78.

molecules. These constants do not refer to a single, well-defined protein state nor imply that only two states are present; they represent a model that we want to test for compatibility with the data. Using eq 2, it is concluded that

$$\frac{d\theta}{dt} = \frac{d\theta_1}{dt} + \frac{k_u}{k_a c}\theta_1 \frac{d\theta_1}{dt} \tag{3}$$

Taking into account that $\theta(t = 0) = 0$ and $\theta_1(t = 0) = 0$, it is found that

$$\theta = \theta_1 + (k_u/2k_a c)\,\theta_1^2 \tag{4}$$

Substituting eq 4 in eq 1 yields

$$\frac{d\theta_1}{dt} = k_a c\left(1 - \theta_1 - \frac{k_u}{2k_a c}\theta_1^2\right) \tag{5}$$

The physical solution of the above equation is

$$\theta_1(t) = \frac{1}{2}\frac{-\frac{2k_a c}{k_u} + \sqrt{\psi} + \left(\frac{2k_a c}{k_u} - \sqrt{\psi}\right)e^{-(k_u/2)\sqrt{\psi}t}}{1 - \left(\frac{2k_a c}{k_u} - \sqrt{\psi}\Big/\frac{2k_a c}{k_u} + \sqrt{\psi}\right)e^{-(k_u/2)\sqrt{\psi}t}} \tag{6}$$

with

$$\psi = \left(\frac{2k_a c}{k_u}\right)^2 + \frac{8k_a c}{k_u} \tag{7}$$

which for $t \to \infty$ reduces to the concentration-dependent final states

$$\theta_1 = -\frac{k_a c}{k_u} + \sqrt{\left(\frac{k_a c}{k_u}\right)^2 + \frac{2k_a c}{k_u}} \tag{8}$$

As expected, $\theta_1 \to 1$ for $k_u \ll k_a c$, indicating that the whole surface area is covered with native proteins. In case of $k_u \gg k_a c$, $\theta_1 \to 0$. The latter behavior reveals the limitations of the model: since no assumptions were made regarding the maximum size of an unfolding protein, the whole surface area may be covered by a single molecule, resulting in vanishing values for θ_1. As this prediction is obviously inconsistent with the real situation, the above model is not applicable for $k_u \gg k_a c$.

In order to compare the measured adsorption kinetics of Figures 7 and 8 to the above model, a relationship between sensor response and θ_1 the number of molecules per unit area, whether native or denatured—has to be found. If mass loading of the crystal surface is assumed to be the relevant parameter, the observed frequency shifts, Δf, will be proportional to this number of adsorbed molecules. The maximum response, Δf_{max}, is obtained for a sensing surface completely covered with native proteins (that is $\theta_1 = 1$). Thus,

$$\Delta f = \Delta f_{max}\theta_1 \tag{9}$$

Fitting the data of Figure 8 with eqs 8 and 9 yields $k = k_a/k_u = (9.79 \pm 0.32) \times 10^{-3}$ mL/μg and $\Delta f_{max} = 0.688 \pm 0.089$ kHz. The underlying procedure used to fit the data to this model was based on the Levenberg–Marquardt algorithm.[25] From eq 8, such value of k results in steady state values of $\theta_1 = 0.22$ and $\theta_1 = 0.86$ for $c = 3$ μg/mL and $c = 280$ μg/mL, respectively. Thus, for the range of concentrations studied, the minimum number of molecules forming a complete monolayer is ~20% of the value that would be obtained if all molecules were in their native state ($\theta_1 = 1$). In other words, fibrinogen covers a surface area 5 times higher than in its native conformation for the extreme case of $c = 3$ μg/mL. As this value is still within the expectation, the model seems to be applicable for all concentrations studied, although $k_u > k_a c$ for $c < 100$ μg/mL. Using the above values of k and Δf_{max} and varying them within the computed errors, k_u is determined by fitting the data of Figure 7 with eqs 6 and 9. The results are summarized in Table 1.

Table 1. Averaged Time Constants Computed for the Experiments Shown in Figure 7[a]

c (μg/mL)	k_u (s^{-1})	$10^3 k_a$ (mL/μg s)
3	0.246 ± 0.039	2.41 ± 0.38
14	0.374 ± 0.032	3.66 ± 0.34
28	0.266 ± 0.017	2.60 ± 0.17
140	0.275 ± 0.017	2.69 ± 0.18
280	0.146 ± 0.009	1.43 ± 0.10

[a] The fit routine used was based on the Levenberg–Marquardt algorithm. It is seen that the values of k_u and k_a fall within the same range, although the variations are higher than the numerical errors.

Although the variations of k_u and k_a at different protein concentrations are higher than the numerically computed errors, all values fall within the same range. It can, therefore, be concluded that the kinetic model is compatible with the experimentally determined adsorption kinetics. A larger set of experiments could probably further reduce inconsistencies. The observed deviations may, however, also be attributed to small differences in the surface properties after each regeneration step or to slightly varying flow conditions in the liquid cell. An optimization of the present flow system should overcome the latter problem. Additional biochemical and spectroscopic experiments will help to determine whether the idealized, two-state system postulated here adequately models the real physical system, in which the native protein could exist in a number of different confirmations on the surface, in which each of these confirmations could decay to a range of denatured states by processes with complex, multistate kinetics, and in which native and denatured proteins interact with one another, both on the surface and in solution.

CONCLUSION

Acoustic plate mode devices have been used to study the adsorption of fibrinogen at hexa(ethylene glycol)-terminated [$HS(CH_2)_{11}(OCH_2CH_2)_6OH$] and methyl-terminated [$HS(CH_2)_{11}CH_3$] SAMs in situ. While no protein adsorption was observed on pristine hexa(ethylene glycol)-terminated surfaces, methyl-terminated SAMs nonspecifically adsorbed high amounts of protein. It was demonstrated that the main portion of adsorbed molecules is irreversibly bound to the methyl-terminated thiol

(25) Press, W. H.; Teokolfky, F. A.; Vettering, W. T.; Flannery, B. P. *Numerical Recipes in C*, 2nd ed.; Cambridge University Press: New York, 1992.

coating. By flushing the sensor with SDS and PBS, the bound proteins were effectively removed. Film quality was guaranteed by IR, XPS, and contact angle measurements.

In a set of concentration-dependent measurements, the limiting sensor response at long times of adsorption was observed to increase as protein concentration was raised. The measured adsorption characteristics are compatible with an approximate, two-state kinetic model which accounts for both the initial binding of native proteins onto the surface and a subsequent unfolding process. Averaged time constants of the two processes were determined and found to be constant within a factor of 2.5 for all concentrations studied. The observed variations may be due to small differences in the properties of the coating and slightly varying flow conditions on the sensing surface during the experiments.

We concluded that acoustic plate mode devices are one tool that can be used to monitor the kinetics of adsorption of proteins at artificial surfaces. Combined with mathematical models, valuable information about the underlying interaction processes can be obtained. In order to improve the performance of this technique, new sensor designs with enhanced signal-to-noise ratio are presently being developed. An optimization of both the flow system and the quality of the coatings should reduce experimental error.

ACKNOWLEDGMENT

The authors thank R. Kohring and A. Lampert for their help in implementing the fitting routines. This work was funded by the Deutsche Forschungsgemeinschaft, the Fond der Chemischen Industrie, and the DAAD. Work at Harvard University was supported by the NIH, Grant GM 30367, and by the NSF, Grant INT-93-13339.

Received for review January 14, 1997. Accepted June 6, 1997.[⊗]

AC970047B

[⊗] Abstract published in *Advance ACS Abstracts*, July 15, 1997.